Effect of the Precipitation of Dissolved $MnCl_2$ on the Low-Temperature Thermal Conductivity of NaCl†

MILES V. KLEIN*
Laboratory of Atomic and Solid State Physics, Cornell University, Ithaca, New York
(Received May 8, 1961)

Low-temperature thermal conductivity measurements were made on NaCl crystals doped with 10^{-4} mole fraction $MnCl_2$. The manganese ions were first quenched into approximate solid solution and then allowed to age at room temperature. Approximate kinetics of the precipitation that resulted were measured by electron spin resonance. There was surprisingly little change in the conductivity during aging; in particular a low-temperature decrease did not appear. The conclusion was that the presence of clusters cannot be invoked to explain the greater than Rayleigh scattering cross section often observed with point defects at low temperatures. The small conductivity changes that did result were: (1) a depression at temperatures near that of the conductivity maximum, and (2) a gradual rise at higher temperatures towards the values obtained with an undoped crystal. These changes were most rapid near the end of the clustering process and suggest a change in the nature of the precipitate at this stage.

INTRODUCTION

MEASUREMENTS of low-temperature thermal conductivity can be used to study the interactions of phonons with defects in insulating crystals. In a previous paper, we described phonon scattering by oxygen-containing anions in NaCl.[1] The cross section was very large and was proportional to the first power of the phonon wave vector. In this paper we describe some experiments that we hoped would further the understanding of scattering by isolated and clustered point defects of a more conventional variety, those that give approximately a Rayleigh scattering cross section.

High-purity insulating crystals exhibit an extremely high thermal conductivity at temperatures of the order of 1/30 the Debye temperature.[2] At lower temperatures, the phonon mean free path is determined by boundary scattering and is long, but few phonons are excited, and the conductivity is low. At higher temperatures, three-phonon umklapp processes become numerous and decrease the mean free path; thus the conductivity is also low. In the intermediate temperature range, the conductivity is extremely sensitive to the presence of small amounts of impurities, and this fact makes an experimental study of the phonon-impurity interaction possible.

The interpretation of experiments on phonon scattering by point defects, i.e., defects of atomic dimensions, has been difficult. The experimental conductivity data show the effects of the scattering processes only after they have been integrated over a range of phonon wavelengths. In addition the data represent the result of several simultaneously present scattering mechanisms, the most important of which are defect scattering, scattering by the boundary, and three-phonon scattering.[2,3]

Sometimes it is possible to "unfold" the effects of the several mechanisms. For example, when one mechanism dominates the scattering, the other mechanisms can often be neglected. This is not so with point defects, for they by themselves seem to give an infinite conductivity. This comes about when the perturbation-theoretic expression for the relaxation time,

$$1/\tau = A\omega^4, \tag{1}$$

is inserted in the equation for the thermal conductivity,[2–4]

$$K(T) = \tfrac{1}{3}\int C(q,T)v^2(q)\tau(q)d^3q. \tag{2}$$

[Here τ is the relaxation time, A a constant depending on the type and concentration of point defects, q the phonon wave vector, ω the phonon frequency, $v(q)$ the phonon group velocity, and $C(q,T)$ the specific heat per normal mode per unit volume. The integration in Eq. (2) also includes a summation over polarizations.] For small q and at all temperatures the integral diverges. This is prevented by invoking other scattering mechanisms, and it is clear that the resulting thermal conductivity will depend upon how this is done.

Recently two methods have been applied with success to experimental data on isotope and "pseudo-isotope" scattering, in which the main perturbation is through a change in mass. Callaway[5] took the relaxation time given by Eq. (1) and combined it with other relaxation times for three-phonon processes and for boundary scattering. The resulting "total" relaxation time had to be corrected, because the normal (wave vector conserving) three-phonon processes do not directly produce thermal resistance, but this correction turned out to be negligible in many cases.

With this model, Callaway obtained a quantitative fit to the data on enriched Ge^{74} and isotopically normal germanium measured by Geballe and Hull.[6] Later, Callaway and von Baeyer[7] were able to use this model

† Work supported in part by the National Science Foundation and the U. S. Atomic Energy Commission.
* Present address: Max Planck Institut für Metallforschung, Stuttgart, Germany.
[1] M. V. Klein, Phys. Rev. **122**, 1393 (1961).
[2] P. G. Klemens, in *Solid-State Physics*, edited by F. Seitz and D. Turnbull (Academic Press, Inc., New York, 1958), Vol. 7, p. 1.
[3] P. Carruthers, Revs. Modern Phys. **33**, 92 (1961).
[4] P. G. Klemens, Proc. Phys. Soc. (London) **A68**, 1113 (1955).
[5] J. Callaway, Phys. Rev. **113**, 1046 (1959).
[6] T. H. Geballe and G. W. Hull, Phys. Rev. **110**, 773 (1958).
[7] J. Callaway and H. C. von Baeyer, Phys. Rev. **120**, 1149 (1960).

to explain the data of Berman and co-workers on the isotope effect in LiF.[8] Another application of this method was made by Toxen,[9] who obtained a successful fit to his data on dilute alloys of silicon in germanium. (He treated Si as an "isotope" of Ge.)

The other method is that of Ziman and co-workers,[8,10] who approximate the solution of the combined Boltzmann equation (containing both three-phonon and defect scattering) by a variational process. This method was used to obtain a good fit to the LiF isotope data,[8] although it does not seem as suitable as Callaway's for use in the temperature region below the conductivity maximum.

In all cases discussed so far, the results of decreasing the isotopic purity appear as a systematic decrease in the conductivity with little or no shift in the position of the maximum. One last experiment of this type that should be mentioned is that of Williams,[11] who studied KCl containing up to 50% KBr in solid solution. His results were not directly compared with theory, but qualitatively they seem to agree.

There is a second type of point defect which produces qualitative as well as quantitative disagreement with Rayleigh scattering [Eq. (1)] predictions. This type of defect appears in lower concentrations than do isotopes, but the individual defect scatters more strongly because in addition to a change in mass, it perturbs the lattice by means of a localized change in force constants.

Typical results in this category are found in the work of Slack on KCl crystals doped with small amounts of $CaCl_2$,[12] and in the work of Pohl on F centers in LiF.[13] The qualitative features of the curves measured by these two workers are the same. The conductivity decrease produced by the impurities is small on the high-temperature side of the maximum, but relatively large on the low-temperature side. This result appears as a progressive shift in the position of the maximum to high temperatures as the impurity content is increased. This behavior, therefore, violates the result predicted for Rayleigh scattering and found for isotopes and pseudo-isotopes. Pohl tried to fit his data with a Callaway-type calculation, but he was unsuccessful.[13]

Various suggestions have been made to explain the extra resistivity occurring at low temperatures. Slack thought that in his case it might be caused by coherent scattering by colloids of precipitated $CaCl_2$ [12]; however, there was no independent evidence that his crystals did in fact contain such colloids. F centers cannot be precipitated and still behave optically as F centers; thus, Pohl's results[13] cannot be explained by a precipitation mechanism. The F centers might be nonrandomly distributed, however, and this could possibly give rise to coherent scattering of long-wavelength phonons. Again, there was no evidence that this was the case with his crystals. A third suggestion was due to Carruthers.[3] It follows from his theory of strain-field scattering by a point defect. The theory suggests a cross section that would give strong Rayleigh scattering at long wavelengths, but would then decrease when the wavelengths become at all comparable to a lattice spacing. The result might be interpretable as an "extra" low-temperature thermal resistivity.

We can list some of the possible causes for this extra resistivity: (i) The cross section for phonon scattering by a single defect is not compatible with Eq. (1). (ii) Equation (1) holds, but coherent scattering of long-wavelength phonons, due to the geometrical arrangement of the defects, gives a different effective cross section. (iii) Equation (1) holds, but somehow the methods used by Callaway and Ziman to successfully compute the conductivity with a high concentration of weakly acting defects break down in situations with low concentrations of strongly acting defects.

MOTIVATION FOR THE PRESENT EXPERIMENT

This experiment was motivated by considerations similar to those of the two preceding paragraphs. We want to understand the real cause of the extra low-temperature resistivity, and in particular we want to know whether this effect is a property of the defects themselves or of their geometrical arrangement in the lattice.

One approach would be to study a system in which the impurities were known to be randomly distributed. This is no problem for isotopes, but it is for defects having a strain field, which are the ones of interest, for it is the strain field that may cause the defects to interact with one another or with imperfections and thus bring about a nonrandom distribution. We have taken the opposite approach and have studied a system known not to be randomly distributed. Of the many possibilities, the system chosen for this study was $NaCl:MnCl_2$.

The manganous ion replaces two sodium ions when dissolved in the NaCl lattice, and thus for each divalent ion in the lattice there is also a positive ion vacancy. Haven[14] made ionic conductivity measurements on this system, which gave some information about the solubility of the Mn ion. Several parts in 10^4 go into solid solution at high temperatures, but it is practically insoluble at room temperature. Further solubility information was learned from electron spin resonance measurements performed first by Schneider and Caffyn.[15] They were able to distinguish the spectrum

[8] R. Berman, P. T. Nettley, F. W. Sheard, A. N. Spencer, R. W. H. Stevenson, and J. M. Ziman, Proc. Roy. Soc. (London) **A253**, 403 (1959).
[9] A. M. Toxen, Phys. Rev. **122**, 450 (1961).
[10] J. M. Ziman, *Electrons and Phonons* (Oxford University Press, New York, 1960), pp. 257–285.
[11] W. S. Williams, Phys. Rev. **119**, 1021 (1960).
[12] G. A. Slack, Phys. Rev. **105**, 832 (1957).
[13] R. O. Pohl, Phys. Rev. **118**, 1499 (1960).
[14] Y. Haven, *Defects in Crystalline Solids* (The Physical Society, London, 1955), p. 261.
[15] E. E. Schneider and J. E. Caffyn, *Defects in Crystalline Solids* (The Physical Society, London, 1955), p. 74.

of precipitated manganese from that of the ions in solution. In this way they verified that the equilibrium room temperature concentration is very low. They found, however, that a nonequilibrium state could be produced by mild quenching. In this state, the ions were in solid solution; subsequent precipitation occurred slowly over a period of several days.

Additional resonance measurements were made by Watkins.[16] He made a detailed analysis of the spectra of various forms of dissolved manganese and then applied this knowledge to a study of the relative intensities of these spectra as a function of temperature. He found three distinguishable environments for the nonprecipitated ion: (1) Completely isolated—no vacancy nearby. (2) Vacancy in nearest-neighbor position. (3) Vacancy in next-nearest-neighbor position. Watkins' data allowed him to compute the energy of situations (2) and (3) relative to situation (1).[17] These results were compared with those from dielectric loss measurements. He obtained excellent agreement.

This system seemed suitable for a study of the effects of precipitation on thermal conductivity. It was sufficiently similar to the $KCl:CaCl_2$ system studied by Slack[12] so that one could hope to make comparisons between results obtained with the two systems. And, most importantly, the magnetic resonance method was at hand for quantitatively determining the state of aggregation in the crystal and for correlating it with the thermal conductivity data.

EXPERIMENTAL

Thermal Conductivity

The technique used in the thermal conductivity measurements has been outlined in reference 1 and has been described in detail elsewhere.[18] Here it will suffice to mention that small temperature differences along the crystal were measured by a combination of carbon resistor thermometers and differential thermocouples.

Electric Spin Resonance

Resonance experiments were performed on a microwave spectrometer designed and built by R. H. Silsbee. It operated at a constant frequency of about 9.3 kMc/sec, the frequency being stabilized by a Pound circuit. Signals reflected from the experimental cavity were detected by a bolometer bridge using radio-frequency bias. The magnetic field was provided by a 6-in. Varian magnet. The resonances were measured by slowly changing the field, the field sweep being linear in magnet current, not in B field. The field was modulated at 35 cps, and the output of the bolometer was detected in phase with the modulation signal. In this way the derivative of the absorption curve was obtained. The absorption curve itself was obtained by passing the derivative signal through an electronic integrator. Relative intensities were measured by tracing the absorption peaks onto paper, cutting them out, and weighing them.

Crystals

The crystal-growing procedure has been described in reference 1 and was used to grow two manganese-doped crystals for the present investigation. Thermal conductivity results on these crystals will be compared with the results for the "pure" crystal of reference 1, crystal C, which was pulled from a melt of chlorine-treated Reagent grade NaCl without intentional dopings. The surface of crystal C was sandblasted with 27-μ abrasive particles to reduce specular phonon reflection in the hope that a true T^3 low-temperature thermal conductivity would thereby be obtained.[13] The two manganese-doped crystals, denoted by A and B, were of the usual size, about $6\times6\times40$ mm^3. Crystal A was grown by doping untreated NaCl with hydrated $MnCl_2$ and then slowly preheating the entire mixture in vacuum before melting. Crystal B was grown from chlorine-treated NaCl powder with an anhydrous $MnCl_2$ doping. (i.e., crystal B received the same treatment as crystal C, plus doping; crystal A received the same treatment as crystal V of reference 1, plus doping.) If the results on the corresponding undoped crystals hold in the presence of manganese dopings, then it can be assumed that in crystal A there was a small quantity of oxygen-containing anions not present in crystal B, but the oxygen content of both crystals can be assumed to be very low, of the order of 3×10^{-7} mole fraction. Manganese concentrations were determined spectrographically on small samples taken from the boules near the center of the thermal conductivity specimens. Results were 6.0 and 8.0×10^{-5} mole fraction on two different specimens for crystal A and 14×10^{-5} mole fraction on one specimen for crystal B. Two samples for magnetic resonance measurements were also cleaved from approximately the same part of the boules as the centers of the thermal-conductivity samples.

Quenching and Aging Processes

The cleaved crystals were annealed at 750°C and cooled slowly to room temperature. The manganese was put into solid solution by a subsequent quenching process, which was done on each crystal separately. It is possible, therefore, that thermal histories during quenching varied slightly from crystal to crystal. Each crystal was first heated for at least $\frac{1}{2}$ hr at 300°C inside an argon-filled quartz tube. The tube was then plunged directly from the furnace into a dry ice, acetone mixture. Our crystals were more heavily doped than those of Watkins and of Schneider and Caffyn, and this rela-

[16] G. D. Watkins, Phys. Rev. **113**, 79 (1959).
[17] G. D. Watkins, Phys. Rev. **113**, 91 (1959).
[18] M. V. Klein, Ph.D. thesis, Cornell University, 1961 (unpublished).

tively fast quenching was needed to produce the unprecipitated state.

The thermal conductivity apparatus did not allow precise control or measurement of temperatures in the vicinity of room temperature. Both samples were mounted in the apparatus once and for all and were left in place with thermometers attached during aging. Ordinarily, because of intentionally poor thermal contact with coolant baths, cooling and warming of the crystals took place slowly. With crystal A no effort was made to obtain rapid initial cooling. It spent a total of 7 hr at room temperature before being cooled to 78°K in preparation for the first conductivity run. Other runs followed, with total room temperature aging times of 60, 103, and 2900 hr.

The initial aging time for crystal B was reduced to approximately $\frac{1}{2}$ hr by using nitrogen exchange gas. For several subsequent conductivity runs, the cooling and warming rates were enhanced by additional use of the exchange gas. The first run was made after aging 30 ± 10 min. The remaining runs followed after total agings of 6, 12.5, 44.5, and 217 hr.

To compute aging times, a critical temperature was arbitrarily taken as 0°C; i.e., at higher temperatures aging was considered to occur at the same rate as at room temperature, whereas at lower temperatures no aging was considered to occur. This procedure could have been improved by knowledge of the precipitation kinetics as a function of temperature, but the necessary measurements were not made. Any reasonable cutoff temperature would yield acceptable results provided that the total transit time from room temperature to low temperatures and back was small compared with the incremental aging time. This condition was satisfied in all cases except possibly the first run with crystal B.

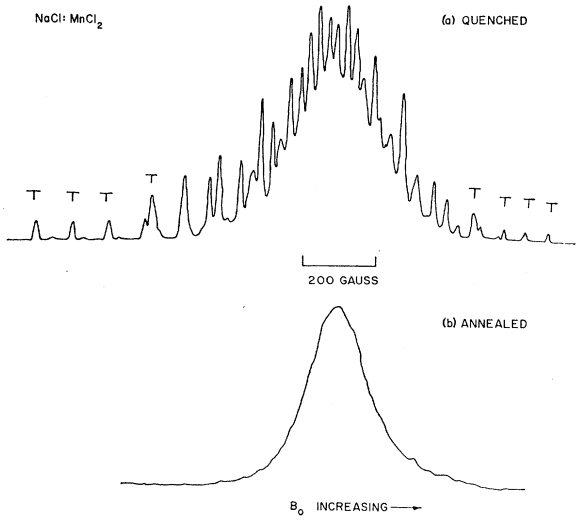

FIG. 1. Resonance spectra for quenched and annealed crystals of NaCl:$MnCl_2$. Those lines in the tails marked with a T were used for quantitative work.

APPROXIMATE PRECIPITATION KINETICS

An estimate of the rate of precipitation of the manganese from solid solution was obtained by means of electron spin resonance measurements. The two resonance samples were quenched and aged together, but independently from the thermal conductivity samples. After quenching, the resonance samples were warmed to room temperature for mounting in the cavity and then cooled back down to dry ice temperature, where the early measurements were made; later measurements were made at room temperature. (Linewidths are temperature independent at these low temperatures; thus, the spectrum was in no way affected by making the measurements at the lower temperature.) The times required for the room-temperature manipulations of the crystals were included in the estimate of the total aging time.

In order to estimate quantitatively the fraction of manganese remaining in solid solution, use was made of Watkins' analysis of the spectrum of NaCl:$MnCl_2$.[16] The ground state of the Mn^{++} ion (electron spin $\frac{5}{2}$) is an S state; thus the energy levels are split only slightly in a cubic field, and the spectrum of an isolated substitutional ion gives six approximately equally spaced hyperfine lines. (Nuclear spin is $\frac{5}{2}$.) This is spectrum II, and it is found at high temperatures. In a quenched specimen at room temperature, only about 10% of the ions are so isolated. The rest are associated with a vacancy at either the nearest- or next-nearest-neighbor position. This produces axial symmetry and gives rise to spectrum III. When the steady magnetic field is along a cube axis, each case involves two nonequivalent types of defects, which split the level in different amounts. The hyperfine multiplet associated with the $\pm\frac{5}{2}\leftrightarrow\pm\frac{3}{2}$ electronic transition is shifted the most, that associated with the $\pm\frac{3}{2}\leftrightarrow\pm\frac{1}{2}$ transition is shifted about half as much, and that associated with the $+\frac{1}{2}\leftrightarrow-\frac{1}{2}$ transition is hardly shifted at all. Thus, the latter spectrum from the 90% of the Mn^{++} present as ion-vacancy pairs (part of spectrum III) is super-

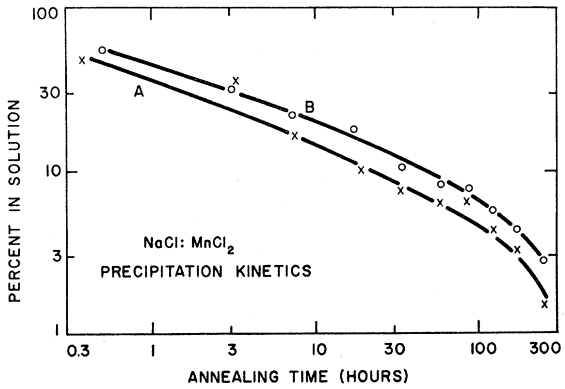

FIG. 2. Precipitation kinetics of $MnCl_2$ in the two NaCl crystals used for thermal conductivity measurements. Annealing took place at room temperature.

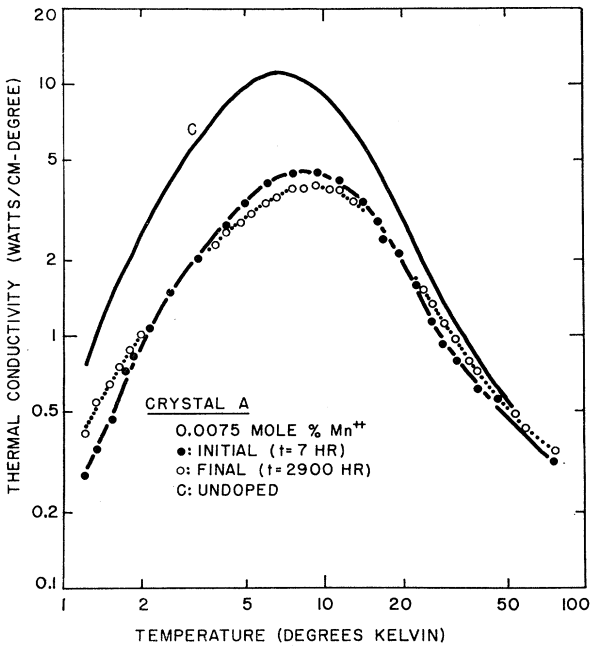

FIG. 3. The over-all effect of $MnCl_2$ precipitation on the thermal conductivity of crystal *A*. Total room temperature annealing times are in parentheses. The approximate fractions of total manganese in solid solution were: initial, 19%; final, <1%.

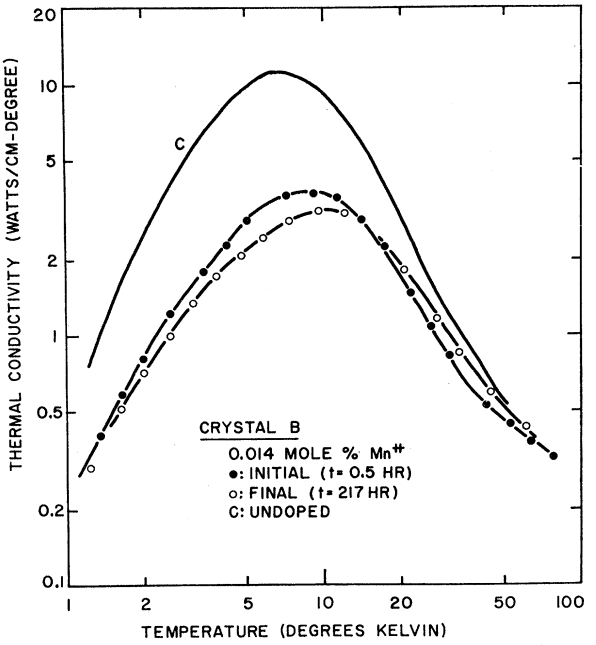

FIG. 4. The over-all effect of $MnCl_2$ precipitation on the thermal conductivity of crystal *B*. Total room temperature annealing times are in parentheses. The approximate fractions of total manganese still in solution were: initial, 55%; final, 3%.

imposed upon the entire spectrum from the 10% of the Mn present as isolated ions (spectrum II). The spectrum of such a quenched crystal is shown in Fig. 1(a).

In a fully annealed specimen, the manganese ions are clustered, and dipole-dipole interaction with nearby spins gives the single broad line shown in Fig. 1(b). With a partially annealed specimen one observes a superposition of Figs. 1(a) and (b), and their relative intensity indicates the fraction of the ions still in solution. Unfortunately, there is sufficient overlapping of the lines in the center of spectrum 1(a) to prevent a direct determination of the amount of spectrum 1(b) present. This difficulty was resolved by identifying the isolated lines in the tails of Fig. 1(a) and determining theoretically what fraction of the total intensity of spectrum III these lines represent. We then multiplied the ratio of the intensity of the lines marked with a *T* in Fig. 1(a) to the total intensity of each measured spectrum by 8.3 to give the "true" intensity ratio, i.e., the fraction of total manganese remaining unclustered.

There were several sources of systematic error in this procedure. Because there was no easy method of resolving the six most prominent lines into spectrum II and spectrum III components, we chose to neglect the former and assumed that all nonclustered manganese ions had a vacancy associated with them. We did include lines belonging to ions with both nearest- and next-nearest-neighbor vacancies. The latter are weak and are barely visible in the low-field tail of Fig. 1(a), between the lines marked with a *T* (which come from the nearest-neighbor configuration).

In addition, we have assumed that the total intensity of the spectrum remained constant during aging, or equivalently, that in spite of the broadening of the individual lines of spectrum III, the integrated intensity did not change. The truth of this assumption was not checked, because from run to run the spectrometer could not be operated under identical conditions of tuning and of sample position in the cavity. Thus the intensity ratio mentioned above may only semiquantitatively be taken as a measure of the fraction of total magnanese still in atomic solution. This is sufficient for our purposes.

The intensities and spacings of the lines in both high- and low-field tails of spectrum 1(a) should be about equal. That they are not can be attributed to the nonlinearity in *B* field of the field sweep. This result could also affect the correct determination of relative intensities. All the spectra were run in the same way, however, and this error would be common to all solubility values.

The results appear in a double logarithmic plot in Fig. 2. The scatter in the data shows that this method of studying precipitation kinetics is not very precise; however, the major trends in the process are indicated.

THERMAL CONDUCTIVITY RESULTS

The over-all changes in thermal conductivity produced by aging the initially quenched NaCl:$MnCl_2$ crystals were small. This can be observed in Figs. 3 and 4. The changes shared by the two crystals are a 10–20% decrease in conductivity in the vicinity of the maximum

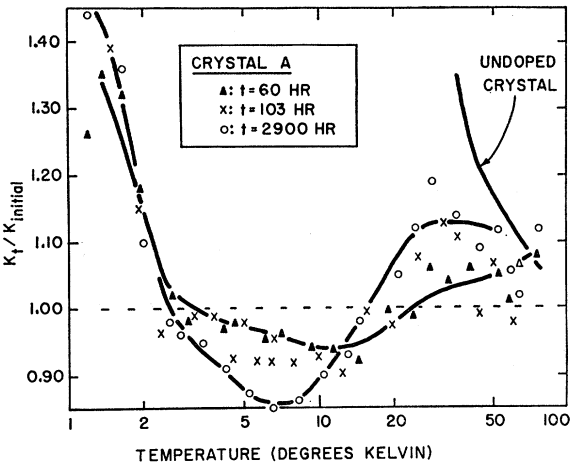

FIG. 5. Details of the change in thermal conductivity with manganese precipitation for crystal *A*. The ordinate is the ratio of the conductivity after *t* hours of annealing to that after 7 hr (Fig. 3). The approximate fractions of total manganese still in solution were 7%, 4.7%, and <1%, for the three curves in order of increasing *t*.

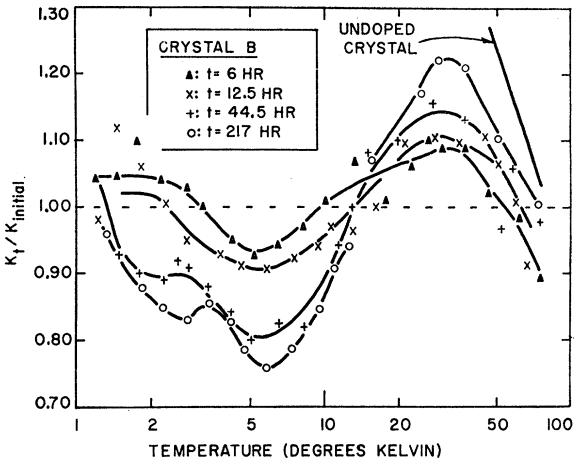

FIG. 6. Details of the change in thermal conductivity with manganese precipitation for crystal *B*. The ordinate is the ratio of the conductivity after *t* hours of annealing to that after 0.5 hr (Fig. 4). The approximate fractions of total manganese still in solution were 25%, 19%, 10%, and 3%, for the four curves in order of increasing *t*.

plus a small rise in conductivity at high temperatures. The low-temperature data for the two crystals disagree, crystal *A* indicating a rise with aging, crystal *B*, a slight decrease. The following discussion will be concerned mainly with the similarities in the results, not the differences.

Since the thermal conductivity changes are small, they are best exhibited as in Figs. 5 and 6, where the ratio of the conductivity after annealing time *t* to that measured initially is plotted for each crystal. The data for crystal *B* are the more accurate, as they were taken later with better technique, but the two sets of data give the same qualitative picture, namely a progressive increase with time of the changes noted above in connection with Figs. 3 and 4. Data for the two crystals are complementary to the extent that the runs made on crystal *B* concentrated on the early stages of the aging, whereas those on *A* emphasized the later stages.

Several features of the results should be pointed out. The first is the systematic approach of the high-temperature conductivity of the annealed crystal to that of an undoped crystal. Therefore, in this region the phonon scattering power per manganese ion is decreasing. Another feature is the progressive decrease in the conductivity maximum. This has the effect of decreasing the slope of the curves at low temperatures.

Also worthy of notice are the stages in the aging process in which the conductivity changes are most rapid. The most rapid changes occur after the greater part of the ions have precipitated. For example, Fig. 6 shows that the relative conductivity near the maximum changes by barely 10% while the approximate fraction of dissolved manganese is decreasing from 55% to 19%, whereas the conductivity changes by 15% while the approximate fraction in solution is decreasing from 19% to 3%. The data of Fig. 5, although not too precise, suggest that after this late rise, the rate of change of conductivity with increasing fraction of clustering levels off (below the point where about 10% are in solution) and finally decreases (below the 1% level).

No information about the size or shape of the clusters can be learned from the magnetic resonance measurements. This is not so with the thermal measurements. Their quantitative response appears not to be a simple function of the fraction precipitated; another factor must be involved. Since the thermal conductivity changes are most pronounced during the later stages of the clustering process, when practically all the ions have precipitated, this factor is probably a change in the nature of existing precipitates.

DISCUSSION

An attempt will now be made to understand the general features of the experimental results. Attention will be directed primarily to (1) the conductivity of undoped NaCl, (2) the general form of the conductivity curve for NaCl:$MnCl_2$, and (3) the effects of manganese precipitation.

The "Pure" Crystal

Crystal *C* was grown from oxygen-free material with no intentional dopings. The question of its defect concentration must now be considered.

Dislocations

Quantitative etch-pit counts were not performed, but a qualitative visual observation was made, which was consistent with a pit density of $10^4/cm^2$–$10^5/cm^2$, the

value observed in undeformed LiF by Sproull *et al.*[19] and in KCl by Slack.[12] Such a dislocation density would not be expected to contribute noticeably to the thermal resistivity (if the results on LiF can be taken to apply to other alkali halides[19]).

Chemical Impurities

In the Appendix of reference 1 it was mentioned that this crystal contained about 50 parts per million calcium and 10 to 100 ppm aluminum. Judging from the results of Slack on $KCl:CaCl_2$,[12] and the present work on $NaCl:MnCl_2$, these concentrations of multivalent impurities would have a marked effect on the thermal conductivity, provided that they were in solid solution. As will be shown below, however, one can give a reasonably good quantitative explanation of curve C without invoking appreciable scattering from these impurities; thus they are presumably not atomically dispersed throughout the crystal and may not even be in ionic form.

Finally, a small amount of scattering could result from whatever oxygen-containing anions were left after the chlorine treatment.

Isotopes

Isotope scattering is thought to be the predominant impurity effect in crystal C. According to Klemens,[4] its contribution to the reciprocal relaxation time is given by Eq. (1) with

$$A=(a^3/4\pi)v^{-3}\Gamma. \tag{3}$$

Here a^3 is the molecular volume, v is the velocity of sound, and Γ is the mean square fractional deviation of the masses of the various isotopic combinations in the unit cell: $\Gamma=\sum_i f_i(\Delta m_i/m_i)^2$, where f_i is the fractional abundance of combination i. For NaCl, $\Gamma=2.17\times10^{-4}$. A was computed using $a^{-3}=2.23\times10^{22}$ cm^{-3} and $v=3.85\times10^5$ cm/sec. The velocity of sound was computed from the Debye temperature using $\theta=320$°K.[20] The result for A was 1.35×10^{-44} sec^3.

Calculation of Conductivity

As mentioned above, there are problems associated with the calculation of the thermal conductivity when the relaxation time is proportional to ω^{-4}. The method of calculation used here is the simple model applied to germanium by Callaway[5] and to LiF by Pohl.[13] With this method the conductivity is calculated from

$$K=\frac{1}{2\pi^2 v}\int_0^{\omega_D}\tau\frac{\hbar^2\omega^4 e^{\hbar\omega/kT}}{kT^2(e^{\hbar\omega/kT}-1)^2}d\omega, \tag{4}$$

where ω_D is the Debye frequency, $\omega_D=k\theta/\hbar$. Here τ is the "combined" relaxation time, whose reciprocal equals the sum of the scattering rates for the various processes. Other scattering processes are provided by three-phonon interactions and the boundary. According to Casimir,[21] the boundary scattering rate is given by v/L with $L=\pi^{\frac{1}{2}}W$. W is the width of the crystal, assumed square. The total three-phonon scattering rate is probably most correctly expressed in the form $[B_1\exp(-\theta/aT)+B_2]\omega^2T^3$; however, the simpler expression, $B\omega^2T^3$, gave reasonable agreement, and it was used instead. The coefficient B was obtained from the measured conductivity at 35°K using an approximate expression for the "high" temperature conductivity derived from Eq. (36) of Callaway's paper[5]:

$$K=k^2/(6\hbar BvT^2).$$

The measured value of W (6.55 mm) did not give a good low-temperature fit to the data; a much better fit resulted from a value 1.6 times larger. This lack of agreement could point to the presence of a significant amount of specular reflection at the crystal surfaces. The surfaces were rough, however, and Pohl obtained quite good agreement with his artificially roughened LiF crystal.[13] Another explanation for the present result could be a lack of exact validity of the Casimir expression for NaCl, perhaps because an "average" sound velocity had not been computed correctly, or because differences between boundary scattering of longitudinal and transverse phonons were not correctly treated.

The total reciprocal relaxation time was obtained by adding the three scattering rates described above. Conductivity curves were calculated by a numerical integration of Eq. (4). The results for different A values appear in Fig. 7. Curve 1 is the curve that would be expected for chemically and isotopically pure NaCl ($A=0$). Curve 2 corresponds to the value of A given by isotope scattering. It agrees reasonably well with the measured curve for the "pure" crystal, but two features should be discussed. The first is the higher conductivity shown by the measured curve for temperatures between 7° and 20°K. The computed curve probably could be made to agree by reinserting a small exponential term in the three-phonon scattering rate. This would make the position of the conductivity maximum coincide more exactly with that of the measured curve. The second feature is the higher low-temperature conductivity of the calculated curve. After the high-temperature adjustment provided by the inclusion of the exponential term, this low-temperature effect would probably make the height of the maximum of the computed curve about 20% higher than that of the measured curve. This fact could be explained by the presence of a small amount of scattering by residual chemical impurities.

[19] R. L. Sproull, M. Moss, and H. Weinstock, J. Appl. Phys. **30**, 334 (1959).

[20] J. A. Morrison, D. Patterson, and J. S. Dugdale, Can. J. Chem. **33**, 375 (1955).

[21] H. B. Casimir, Physica **5**, 495 (1938).

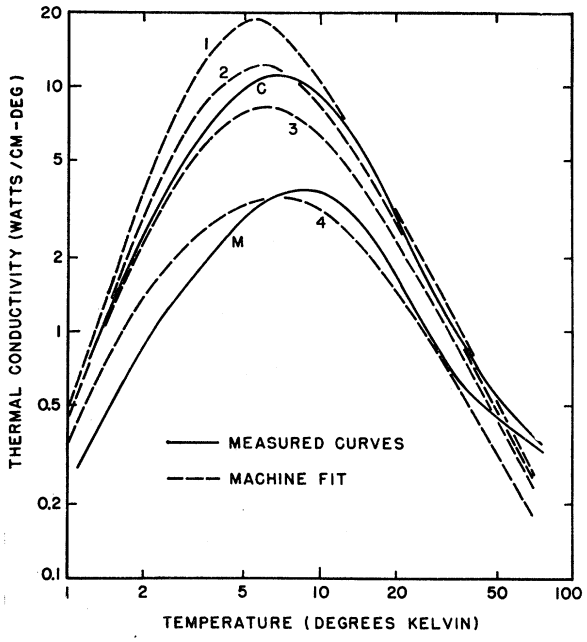

FIG. 7. Comparison of measured thermal conductivity curves of pure (*C*) and $MnCl_2$-doped (*M*) NaCl with computed curves. The curves were computed for various amounts of Rayleigh scattering (additive scattering rate $=A\omega^4$). The value of A, in units of 10^{-44} sec^3, for the various curves is: curve 1, $A=0$; curve 2, $A=1.35$; curve 3, $A=4.90$; curve 4, $A=30$.

General Features of the Conductivity of NaCl:$MnCl_2$

Curve *M* in Fig. 7 is the initially measured conductivity of crystal *B*. It should be compared with curve 4, which was calculated for a value of A of 30×10^{-44} sec^3. The order of magnitude agreement is good, but, as was found with the pure crystal, there are some qualitative discrepancies. In this case, however, the high-temperature disagreement is too great to be repaired by the use of the same exponential term that would probably give agreement for the pure crystal. Curve 4 would still be below curve *M* at high temperatures and above curve *M* at low temperatures. A Rayleigh scattering cross section as used with the Callaway model does not seem to produce detailed agreement with experiment; the actual defects apparently scatter more strongly at low temperatures. This is exactly the behavior observed in[12] KCl:$CaCl_2$ and in[13] LiF with *F* centers, the earlier work that motivated the present investigation.

Although the shape of curve 4 does not agree precisely with experiment, its magnitude may be a significant quantity. Equation (3) was generalized by Klemens[4] to include other Rayleigh scattering processes by writing

$$A=(3a^3/\pi v^3)S^2F, \tag{5}$$

where S^2 is the dimensionless parameter that describes the strength of the scattering, and F denotes the fractional concentration of the impurity. For mass scattering, $S^2=\Gamma/12$ with $F=1$; for scattering by a change in atomic linkages, Klemens estimated the contribution to S^2 to be $\frac{1}{6}(\Delta f/f)^2$; and for scattering due to a change in linkages accompanied by a distortion of the lattice the contribution was $24(\Delta R/R)^2$. The nearest-neighbor distance is denoted by R, and the force constant by f. Another calculation is that of Carruthers, who estimated the strength of the Rayleigh scattering by the strain field around a point defect.[3] His result is $(\pi/3)75\gamma^2\epsilon^2$. Here γ is Grüneisen's constant and equals about 1.6 for NaCl; the parameter ϵ gives the fractional amount of volume misfit for the impurity ion relative to the lattice ion.

The value of A for curve 4 corresponds to a value of 2.9 for S^2 at the concentration of manganese in crystal *B*. This result is much greater than that expected from mass scattering. At long phonon wavelengths it is the mass change averaged over several unit cells that appears in Δm. Since most of the manganous ions have a vacancy nearby, the proper Δm to take is that of one $MnCl_2$ molecule with respect to two NaCl molecules. In this case, $\Delta m/m$ is about 0.08, and S^2 is three orders of magnitude too small. Since $(\Delta f/f)^2$ cannot reasonably be much larger than unity, the predicted scattering from atomic linkages is also too small. As for the effect of lattice distortion, a 30% fractional change of R would be needed, according to Klemens, to give an S^2 of 2.9. This would correspond to a 100% change in volume and seems somewhat high.

Agreement is obtained with Carruthers' strain field scattering estimate using a fractional volume misfit of 0.12, not unreasonable. His model, therefore, gives the best agreement. This conclusion is quite weak, for it ignores two important considerations. The first has been mentioned above, namely, the difference in shape between the theoretical and experimental curves and its implication in terms of a non-Rayleigh scattering mechanism. The second consideration is the likelihood that about half of the manganese had already precipitated by the time of the conductivity measurement. This is the conclusion drawn from the spin resonance results shown in Fig. 2. The above quantitative estimates would require revision before being applicable to clusters.

Changes Accompanying Manganese Precipitation

The observed thermal conductivity changes were discussed in connection with Figs. 3 through 6. The outstanding single feature of all the data is the low-temperature behavior, which does not exhibit any sizeable decrease upon annealing; in fact, crystal *A* exhibits an increase. Thus, there is no empirical evidence that the lack of agreement (between the prediction based on Rayleigh scattering and the extra low-temperature resistivity observed experimentally) is attributable to phonon scattering by clusters. This does not mean,

however, that clusters are definitely *not* responsible for the anomaly, because measurements could not be made during the very early stage of the clustering process. It is possible that this early stage was accompanied by the appearance of the extra low-temperature resistivity, which quickly saturated, or even decreased, during the later stages of clustering. The data give no hint of such a process, however, and thus it seems that the cause of the anomaly must lie elsewhere.

The actually observed changes upon aging are difficult to explain. Unfortunately, there is no independent information about the size and shape of the precipitates, as might be obtained by x-ray or electron microscope studies. Miyake and Suzuki have studied a related system produced by doping NaCl with a few percent $CaCl_2$.[22,23] These authors studied x-ray diffraction patterns of the heavily doped crystals that indicated the presence of disk-shaped precipitates, 10–20 A thick and 100–200 A long oriented normal to the [111] and [310] directions. This suggests that disks might also be found in the manganese-doped crystals.

A disk-shaped precipitate is also suggested by the crystal structure of pure $MnCl_2$. The lattice can be considered as formed from a face-centered cubic, close-packed, Cl^- lattice that has the layers of octahedral voids between the close-packed planes alternately filled with Mn^{++} ions and empty.[24] This structure would be obtained by removing every other close-packed layer of Na^+ in NaCl and replacing the remaining positive ions with Mn^{++}. The resulting layer structure corresponds to a noncubic distortion of the NaCl lattice having a 7% higher lattice constant.

It may be possible for the $MnCl_2$ precipitates to grow in layers having the structure of pure $MnCl_2$, but distorted somewhat, lying in close-packed planes of the host lattice and in registry with them. With a precipitate density at all like that of the bulk material, one would expect that the host lattice would have to close the gap left by the atomically more dense precipitate by displacing itself in a direction normal to the precipitate plane. The strain field resulting from this displacement would be similar to that of a dislocation loop.

An additional scattering process, which would take place even in the absence of a strain field, would result from a change in sound velocity in the precipitate as compared with the host lattice. To make a realistic estimate of the scattering cross section resulting from these two processes would require a major effort, particularly for phonon wavelengths comparable with the size of the precipitate.

We pointed out earlier that the experiments suggest a change in the nature of the precipitate during the later stages of the aging process. One explanation of this is that initially the clusters are too small to be stable and are continually evaporating and reforming from the "vapor" of surrounding point defects. Details of this process can be obtained from discussions of nucleation.[25] The small size of these "embryos" might explain why the aging-induced conductivity changes were so small.

The more rapid late conductivity changes may be an indication of the appearance of a stable precipitate. This would occur when the "vapor pressure" of the point defects and embryos would become sufficiently great to enable some stable clusters to form.

SUMMARY

(1) The low-temperature thermal conductivity of quenched NaCl:$MnCl_2$ was found to be qualitatively similar to that found in KCl:$CaCl_2$ and LiF containing *F* centers; it cannot be explained in detail by a Callaway-type calculation using a Rayleigh scattering cross section.

(2) Nevertheless, rough quantitative agreement was obtained, which suggested, albeit weakly, that strain-field scattering was the primary scattering mechanism for "isolated defects."

(3) The changes observed during clustering of $MnCl_2$ were small and rule out the interpretation of the discrepancy in item (1) being caused by coherent scattering by precipitates. This strengthens the belief that the above discrepancy is an inherent property of the atomically dispersed defects.

(4) The conductivity results suggest the onset of a new stage in the precipitation process after most of the ions have clustered.

ACKNOWLEDGMENTS

The author wishes to express his gratitude to Professor R. L. Sproull for his guidance throughout this investigation, to Professor R. O. Pohl for many interesting suggestions and discussions, to Professor R. H. Silsbee for help with the magnetic resonance measurements, and to Mr. J. Ashe for growing the crystals. He is also grateful to the National Science Foundation for fellowship support during the early part of this work.

[22] S. Miyake and K. Suzuki, J. Phys. Soc. Japan **9**, 702 (1954).
[23] K. Suzuki, J. Phys. Soc. Japan **10**, 794 (1955).
[24] R. G. Wyckoff, *Crystal Structures* (Interscience Publishers, Inc., New York, 1951), Vol. 1, Chap. IV, p. 21.
[25] R. Smoluchowski, in *Phase Transformations in Solids* (John Wiley & Sons, Inc., New York, 1951).